Computación y Sistemas Número Especial pp. 158 - 165
© 2002, CIC - IPN. *ISSN 1405-5546* Impreso en México

Extracting Transmission (S_{21}, S_{12}) Parameters of Two-Port Devices Embedded in Nonreflecting Lines

Determinación de los Parámetros de Transmisión (S_{21}, S_{12}) de Dispositivos de Dos Puertos Montados en Líneas de Transmisión no Reflectoras

J. Apolinar Reynoso Hernández
Centro de Investigación Científica y de Educación Superior de Ensenada (CICESE)
División de Física Aplicada, Km. 107 carretera Tijuana-Ensenada, B.C., México CP. 22860
E-mail: apolinar@cicese.mx

Article received on June 19, 2001; accepted on February 19, 2002

Abstract

A straightforward broadband method for extracting the S_{21} and S_{12} transmission parameters of devices embedded in nonreflecting transmission lines (microstrip or coplanar) is presented. Two nonreflecting transmission lines (L-L method) or a line and a match (L-M method) are used as standards where one line should be twice as long as the lines into which the device is embedded. Two different procedures for de-embedding S_{21} and S_{12} are investigated. The first one uses the travelling wave vector λ instead of the wave propagation constant γ of the standard line. The second one, based on a novel matrix approach, uses some parameters of the input transition instead of the wave propagation constant γ or the travelling wave vector λ of standard lines. The performance of this method is shown by the broadband measurement of S_{21} and S_{12} of a PHEMT transistor NE24200 (biased at V_{ds} = 2 V; V_{gs} = 0 V) in the frequency range of 45 MHz-50 GHz and by the determination of the small signal-gain of the commercially available SiGe RFIC model SGA-5386 and SGA-5389 in the frequency range of 45 MHz-10 GHz.

Key Words: *de-embedding, Calibration, PHEMTs, Test fixtures, Scattering-parameter, Network Analyzers.*

Resumen

En este artículo se presenta un método de "de-embedding" para determinar los parámetros de transmisión S_{21} y S_{12} de cualquier cuadripolo: activo o pasivo. El nuevo método es implementado utilizando dos líneas (coplanares, microcinta,etc) no refelctoras (metodo L-L) y una línea no reflectora y una carga (Metodo L-M). Se presentan dos procediminetos matemáticos para calcular los parámetros S_{21} y S_{12}. El primer procedimiento se basa en las propiedades de los determinantes y utiliza para efectuar el calculo de S_{21} y S_{12} el vector de onda λ en lugar de la constante de propagación γ de las líneas en las que el dispositivo se encuentra montado. El sengundo método para calcular S_{21} y S_{12}, desarrollado en base a un cálculo matricial original, utiliza el conocimiento parcial de los elementos de la transición TA en lugar del vector de onda λ y la constante de propagación γ. La utilidad del método se demuestra con la medición de los parámetros de transmisión de un transistor PHEMT NE24200 (polarizado a V_{ds} = 2 V; V_{gs} = 0 V) en el intervalo de frecuencia de 40MHz-50GHz y por la determinación de la ganancia en pequeña señal del amplificador comercial SiGe RFIC modelo SGA-5386 y SGA-5389 en el intervalo de frecuencia de 45 MHz-10 GHz.

Palabras Clave: Substracción, Calibración, Transistor Pseudomorfico de Alta Movilidad, Soporte de Pruebas, Medición de Parámetros de Dispersión, Analizador de Redes.

I Introduction

Non-coaxial devices *e.g.* chip transistors, chip amplifiers, *etc.* have to be mounted in a test fixture to be measured. A classical test fixture is formed with two nonreflecting lines (microstrip or coplanar) and two adapters (coaxial connectors or coplanar to microstrip transitions). The test fixture and the Device Under Test (DUT) are shown in Fig. 1. In order to make a full extraction of the DUT scattering parameters S_{ij} from the scattering parameters measured at the connectors plane of the test fixture (see Fig. 1), line wave propagation constant γ and adapters S parameters are needed. Calibration techniques such as *Line-Reflect-Line LRL* (Engen and Hoer, 1979) allow the determination of γ and the adapters S parameters. These error correction techniques use at least three calibration standards. Classical *LRL* (*TRL*) is frequency limited by the line electrical length θ (20° < θ < 160°). This drawback can be overcome if lossy line (Marks R.B, 1991) along with a broadband computation of γ (Reynoso-Hernández J.A, Estrada-Maldonado C. F, 1999) are used.

On the other hand, utilizing the Thru-Line method, Wan(Wan CH, et al 1998) has shown that two line standards are enough for extracting S_{21} and S_{12} transmission parameters without the previous knowledge of the adapters' S parameters (Wan CH, et al 1998). However, the use of two lines as reported by (Wan CH, et al 1998), does not allow a broadband de-embedding of transmission parameters. This is because phase discontinuities occurs when γ is computed with [Wan CH, et al 1998, Eq.(4)] or [Lee M.Q et al, Eq.(12)] and then these equations do not operate in a broadband frequency range as suggested by (Reynoso-Hernández J.A, Estrada-Maldonado C. F, 1999). The purpose of this work is to investigate whether two standards are still enough for determining S_{21} and S_{12} of the two-port devices mounted in test fixtures with lines of arbitrary length. Moreover, the problem of frequency restrictions is also considered. Using "long lines" a broadband de-embedding method is presented for transmission S_{21} and S_{12} parameters of any two-port device either active or passive, without frequency restrictions and without the previous knowledge of adapters' S parameters.

This article is organized as follows: in section II, the L-L method is presented and in section III a straightforward procedure for determining S_{21} and S_{12} is presented. Experimental results and discussion are given in section IV. Finally, conclusions are drawn in section V.

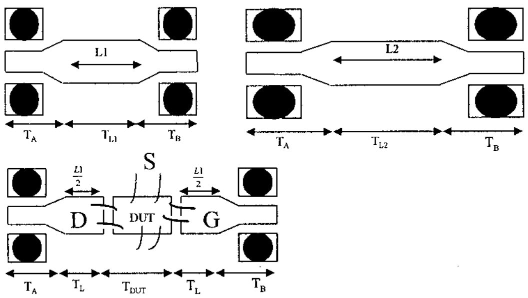

Fig. 1. Layout of the calibrations standards (line L1 and line L2) and the test fixture utilized in the method

2 Extraction of S_{21} AND S_{12} Utilizing Two Nonreflecting Lines

The *L-L* (Line-Line) method needs for its implementation two nonreflecting lines and a device embedded in two lines. The line standards used are shown in Fig. 1. The shorter and longer lines will be referred to as L_1, and L_2 respectively. The two ports referenced as T_A and T_B correspond to transitions used for insuring the connection between the lines and the network analyzer at the line input and output ports. T_A and T_B include either the microwave probes or coaxial to microstrip microwave connectors (launchers) and the necessary hardware for the network analyzer.

Wave Cascading Matrix, WCM, are used for the modeling of transitions T_A, T_B, line L_1 and line L_2. The WCM is defined as: $\mathbf{T_A}$ for transition T_A, $\mathbf{T_B}$ for transition T_B, $\mathbf{T_{L1}}$ for line L_1, and $\mathbf{T_{L2}}$ for line L_2. In the following, $\mathbf{T_A}$ and $\mathbf{T_B}$ are assumed to be different. The three WCM $\mathbf{T_1}$, $\mathbf{T_2}$, and $\mathbf{T_3}$ ($\mathbf{T_1}$ for line L_1 plus transitions, $\mathbf{T_2}$ for line L_2 plus transitions, $\mathbf{T_3}$ for device under test embedded in transitions and lines) can be written as

$$\mathbf{T_1} = \mathbf{T_A}\ \mathbf{T_{L1}}\ \mathbf{T_B}, \qquad (1)$$

$$\mathbf{T_2} = \mathbf{T_A}\ \mathbf{T_{L2}}\ \mathbf{T_B}, \qquad (2)$$

$$\mathbf{T_3} = \mathbf{T_A}\ \mathbf{T_L}\ \mathbf{T_{DUT}}\ \mathbf{T_L}\ \mathbf{T_B}, \qquad (3)$$

where

$$\mathbf{T_{Li}} = \begin{pmatrix} e^{-\gamma Li} & 0 \\ 0 & e^{\gamma Li} \end{pmatrix} \quad i = 1, 2, \qquad (4)$$

$$\mathbf{T_L} = \begin{pmatrix} e^{-\gamma \frac{L_1}{2}} & 0 \\ 0 & e^{\gamma \frac{L_1}{2}} \end{pmatrix}, \qquad (5)$$

$$\mathbf{T_{DUT}} = \frac{1}{S_{21}} \begin{pmatrix} -\Delta S & S_{11} \\ -S_{22} & 1 \end{pmatrix}, \qquad (6)$$

$$\mathbf{T_A} = r_{22} \begin{pmatrix} a & b \\ c & 1 \end{pmatrix}. \qquad (7)$$

$\mathbf{T_{Li}}$ (i = 1, 2) is the WCM of a non reflective line having a length L_i, $\mathbf{T_L}$ is the WCM of a non reflective line having a length $L_1/2$, $\mathbf{T_{DUT}}$ is the WCM of the device under test and $\Delta S = S_{11}S_{22} - S_{12}S_{21}$.

2.1 Computation of S_{21} and S_{12} Using the Wave Propagation Vector λ

(Reynoso-Hernández J.A, Estrada-Maldonado C. F, 2000)

Using (1)-(3) and knowing that the determinant of product matrices is equal to the product of the matrix determinants, the following equations are derived (Wan CH, et al 1998)

$$\frac{\det(T_3)}{\det(T_1)} = \frac{S_{12}}{S_{21}}, \qquad (8)$$

$$\frac{\det(T_1 + T_3)}{\det(T_1)} = \det(T_{L_1} + T_L T_{DUT} T_L), \qquad (9)$$

$$\frac{\det(T_2 + T_3)}{\det(T_1)} = \det(T_{L_2} + T_L T_{DUT} T_L). \qquad (10)$$

Using (4)-(6) and (8), equation (9) and (10) are expressed in matrix form by

$$\begin{bmatrix} p \\ q \end{bmatrix} = \begin{bmatrix} 1 & -1 \\ \frac{1}{\lambda} & -\lambda \end{bmatrix} \begin{bmatrix} 1/S_{21} \\ \Delta S/S_{21} \end{bmatrix}, \qquad (11)$$

where

$$p = \frac{\det(T_1 + T_3) - \det(T_3)}{\det(T_1)} - 1,$$

$$q = \frac{\det(T_2 + T_3) - \det(T_3)}{\det(T_1)} - 1,$$

and $\lambda = e^{\gamma(L_2 - L_1)}$ (11bis).

Solving (11) for S_{21} and (8) for S_{12}, we have

$$S_{21} = \frac{1-\lambda^2}{\lambda(q-\lambda p)}, \tag{12}$$

$$S_{12} = \frac{\det(T_3)}{\det(T_1)} \frac{1-\lambda^2}{\lambda(q-\lambda p)} . \tag{13}$$

It should be noted that when $\lambda^2 = 1$, (12) and (13) remain undetermined quantities. This occurs when angle (λ) = k•180°, k = 0, 1, 2,..., n and line losses are zero (Ln(abs(λ)) = 0 since abs(λ) = 1). However, due to line losses, abs(λ) ≠ 1, and uncertainties in the computation of S_{21} and S_{12} are reduced at some specific frequencies for which angle(λ) = k•180°, k = 0, 1, 2, ..., n. As an example of this problem we plot in Fig. 2. the numerator and denominator of S_{21} . Notice from this ~~plot~~ that both numerator and denominator of S_{21} exhibit a set of three minimums (close to zero but always above to zero) corresponding at electrical length of π, 2π and 3π. Furthermore, as frequency increases, these minimums increases. This behavior could be attributed to the line losses.

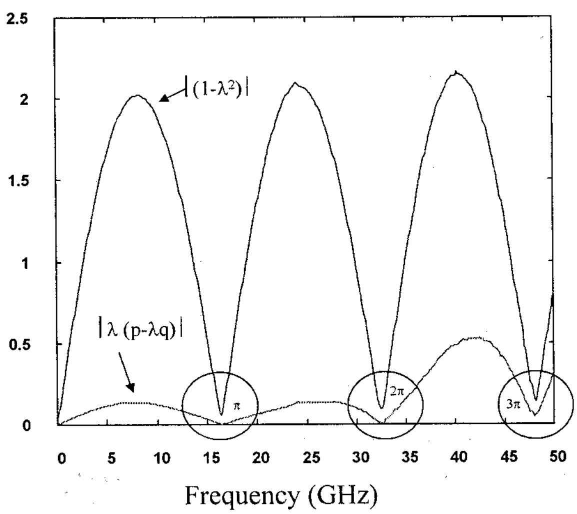

Fig. 2 Plot of numerator and denominator of S_{21} given by Eq. 12 versus frequency

2.1.1 Computation of the Travelling Wave Vector λ

(Reynoso-Hernández,J.A, Estrada-Maldonado C.F,2000)

The travelling wave λ is derived from (1), (2), (4), and (7) using the next procedure.

$$\mathbf{T_X} = \mathbf{T_A^{-1}}\ \mathbf{T}\ \mathbf{T_A}, \tag{14}$$

$$\mathbf{T_X} = \mathbf{T_{L2}}\ \mathbf{T_{L1}^{-1}} = \begin{pmatrix} \frac{1}{\lambda} & 0 \\ 0 & \lambda \end{pmatrix}; \lambda \in C, \tag{15}$$

$$\mathbf{T} = \mathbf{T_2}\ \mathbf{T_1^{-1}} = \begin{pmatrix} t_{11} & t_{12} \\ t_{21} & t_{22} \end{pmatrix}; t_{ij} \in C, \tag{16}$$

Using (14)-(16), equation (14) becomes

$$\begin{pmatrix} \frac{1}{\lambda} & 0 \\ 0 & \lambda \end{pmatrix} = \frac{1}{a-bc} \begin{pmatrix} a(t_{11} + \frac{c}{a}t_{12} - bt_{21} - b\frac{c}{a}t_{22}) & bt_{11} + t_{12} - b^2 t_{21} - bt_{22} \\ a^2(-\frac{c}{a}t_{11} - (\frac{c}{a})^2 t_{12} + t_{21} + \frac{c}{a}t_{22}) & a(-b\frac{c}{a}t_{11} - \frac{c}{a}t_{12} + bt_{21} + t_{22}) \end{pmatrix} \tag{17}$$

Comparing each term of matrices on both sides of (17), λ is computed as a function of b and a/c by

$$\lambda = \frac{t_{22} + bt_{21} - \frac{b}{a/c}t_{11} - \frac{1}{a/c}t_{12}}{1 - \frac{b}{a/c}} = \frac{1 - \frac{b}{a/c}}{t_{11} + \frac{1}{a/c}t_{12} - bt_{21} - \frac{b}{a/c}t_{22}}$$

(18)

where

$$b^2 t_{21} + b(t_{22} - t_{11}) - t_{12} = 0, \tag{19}$$

$$\left(\frac{a}{c}\right)^2 t_{21} + \frac{a}{c}(t_{22} - t_{11}) - t_{12} = 0. \tag{20}$$

It should be noticed that quadratic equations (19) and (20) have already been reported by (Engen and Hoer, 1979) but their derivation is different in this work. On the other hand, because of equal coefficients observed on (19) and (20), b and a/c are roots of the same equation. Moreover, since T_A^{-1} exists $(a - bc \neq 0)$, then b is different from a/c and hence b and a/c are the two different roots of (19) and (20). Values of b and a/c are chosen in accordance to the criterion reported on (Engen and Hoer, 1979).

3 Straightforward Determination of S_{21} and S_{12}

Using (1) and (3), the following equations are derived

$$\mathbf{T}_{\mathbf{DUT}}\ \mathbf{T}_{\mathbf{L1}}^{-1} = \mathbf{T}_{\mathbf{A}}^{-1}\ \mathbf{T}_{\mathbf{3}}\ \mathbf{T}_{\mathbf{1}}^{-1}\ \mathbf{T}_{\mathbf{A}}\ . \qquad (21)$$

Now defining

$$\mathbf{T}_{\mathbf{3}}\ \mathbf{T}_{\mathbf{1}}^{-1} = \begin{pmatrix} p_{11} & p_{12} \\ p_{21} & p_{22} \end{pmatrix}, \qquad (22)$$

$$\mathbf{T}_{\mathbf{DUT}}\ \mathbf{T}_{\mathbf{L1}}^{-1} = \frac{1}{S_{21}} \begin{pmatrix} -\Delta S & S_{11} e^{-\gamma L_1} \\ -S_{22}\ e^{\gamma L_1} & 1 \end{pmatrix}. \qquad (23)$$

On the other hand, from (21) it should be notice that, $\mathbf{T}_{\mathbf{DUT}}\ \mathbf{T}_{\mathbf{L1}}^{-1}$, and $\mathbf{T}_{\mathbf{3}}\ \mathbf{T}_{\mathbf{1}}^{-1}$ are similar matrices and as a result they have the same *determinant*, ($\Delta p = p_{11}\ p_{22} - p_{12}\ p_{21}$) that is,

$$\Delta p = \frac{S_{12}}{S_{21}}\ . \qquad (24)$$

To separate S_{21} or S_{12} from (24) we need an additional expression. This expression is derived by putting (7) and (22) in (21) and expressed as

$$\mathbf{T}_{\mathbf{A}}^{-1}\mathbf{T}_{\mathbf{3}}\mathbf{T}_{\mathbf{1}}^{-1}\mathbf{T}_{\mathbf{A}} = \frac{1}{a-bc}\begin{pmatrix} a\,(p_{11}+\frac{c}{a}p_{12}-b\,p_{21}-b\,\frac{c}{a}p_{22}) & b\,p_{11}+p_{12}-b^2\,p_{21}-b\,p_{22} \\ a^2\,(-\frac{c}{a}\,p_{11}-(\frac{c}{a})^2\,p_{12}+p_{21}+\frac{c}{a}p_{22}) & a\,(-b\frac{c}{a}p_{11}-\frac{c}{a}\,p_{12}+b\,p_{21}+p_{22}) \end{pmatrix} \qquad (25)$$

S_{21} is derived putting (23) and (25) in (21) and comparing each term of matrices on both sides. Finally S_{21} and S_{12} are expressed as

$$S_{21} = \frac{1-\dfrac{b}{a/c}}{p_{22}+bp_{21}-\dfrac{1}{a/c}p_{12}-b\dfrac{1}{a/c}p_{11}}\ , \qquad (26)$$

$$S_{12} = \Delta p\ S_{21}\,. \qquad (27)$$

It should be noted that for computing S_{21} and S_{12} using (26) and (27) we need the *a/c* and *b* values. As it can see, this procedure for deriving S_{21} and S_{12} indicates that the line parameters γ and λ are not needed. In other words, this procedure only needs the partial knowledge of the transition T_A alone. Regarding the *a/c* and *b* values, they can be determined using. (19) and (20) or using Eq.1 and a broadband 50 Ohms load, that is, the "long line" is replaced by a broad band load as in the Line reflect Match calibration technique (Eul H.J, et al, 1988).

3.1 Computation of *a/c* and *b* Using a L-M (Line - Broad Band Match) Method

An alternative way for determining *b* and *a/c* terms is using a nonreflecting line, Eq.1, and a broadband 50 Ohms load. From Eq.1 and solving for matrix $\mathbf{T_B}$, we have

$$\mathbf{T}_{\mathbf{B}} = [\mathbf{T}_{\mathbf{A}}\,\mathbf{T}_{\mathbf{L1}}]^{-1}\,\mathbf{T}_{\mathbf{l}} \qquad (28)$$

Defining $\mathbf{T_1}$ as (Marks R.B, 1991)

$$T_1 = g\begin{pmatrix} d & e \\ f & 1 \end{pmatrix}. \qquad (29)$$

Using Eq.4 and Eq.5 the matrix $\mathbf{T_B}$ given by (28) becomes

$$T_B = \rho_{22}\begin{pmatrix} \alpha & \beta \\ \varphi & 1 \end{pmatrix}, \qquad (30)$$

where

$$\rho_{22} = \frac{(1-\frac{c}{a}e)}{(1-\frac{c}{a}b)}\frac{g}{r_{22}}e^{-2\gamma L_1}\,, \qquad (31)$$

$$\alpha = \frac{(d-bf)}{a\,(1-\frac{c}{a}e)}e^{2\gamma L_1}\,, \qquad (32)$$

$$\beta = \frac{(e-b)}{a\,(1-\frac{c}{a}e)}e^{2\gamma L_1}\,, \qquad (33)$$

$$\varphi = \frac{(f-\frac{c}{a}d)}{(1-\frac{c}{a}e)}\,, \qquad (34)$$

It should be noted from Eq.34 that *c/a* can be easily determined if φ is known since *f*, *d* and *e* are elements of

$\mathbf{T}_1$ matrix and all of them are known. Then solving for *c/a* from Eq.34, we have

$$\frac{c}{a} = \frac{(\varphi\, e - 1)}{(\varphi - f)}\,, \qquad (35)$$

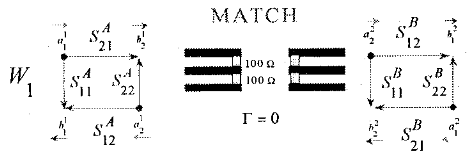

Fig. 3 Error model for transition T_A and T_B used for computing *b* and *a/c*

On the other hand, modeling the transition T_A and T_B as shown in Fig.3, *b* and φ values can be easily determined using a broad-band load (50 Ohms). The reflection coefficient W_1 and W_2, measured as a function of reflection coefficient Γ_L are given as

$$W_1 = S_{11}^A + \frac{S_{12}^A S_{21}^A \Gamma_L}{1 - S_{22}^A \Gamma_L} = \frac{a\,\Gamma_L + b}{c\,\Gamma_L + 1}\,, \qquad (36)$$

$$W_2 = S_{22}^B + \frac{S_{12}^B S_{21}^B \Gamma_L}{1 - S_{11}^B \Gamma_L} = \frac{\alpha\,\Gamma_L - \varphi}{1 - \beta\,\Gamma_L}\,. \qquad (37)$$

Assuming that the refletion coefficient Γ_L of the broad-band load is equal to zero (perfectly matched), the *b* and φ values are expressed as

$W_1 = b$,

$W_2 = -\varphi$.

Notice that $b = S_{11}^m$ and $\varphi = S_{22}^m$; S_{11}^m y S_{22}^m are the scattering parameters measured when transitions are loaded with a broadband match. Once φ is computed the *a/c* term is determined using Eq.35.

The main advantage in the determination of *b* and *a/c* terms using a broadband load is that the difficulty in to discern *b* and *a/c* is eliminated. Furthermore, the condition that lines have to be lossy can be lifted.

4 Results

In order to show the usefulness of the proposed L-L and L-M methods, measurements were performed on PHEMTs (NE24200 with W_g = 200 μm and L_g = 0.25 μm) and RFIC amplifiers (SGA5386 and SGA5389).

Prior to scattering parameters measurements, a two-tier calibration was performed on a HP8510C network analyzer in the frequency range of 0.045-50 GHz. The first tier calibration is performed with the SOLT calibration technique using a coaxial calibration kit from HP. With this calibration, the systematic errors of the network analyzer are achieved. The second tier calibration is performed using the *L-L, L-M* and the multilines *LRL* (Marks R.B, 1991) calibration techniques implemented using coplanar-microstrip structures from a calibration *kit ProbePoint*™ CMO5. The S_{21} and S_{12} parameters of a PHEMT transistor de-embedded with the multiline method were used as verification elements of calibrations. The transistor was mounted in a coplanar test fixture formed with two 50 ohms coplanar to microstrip transitions supplied by *JCmicrotechnology* . Details of this test fixture are indicated in Fig. 1. Regarding the λ computation, Fig. 4 shows the broadband variations in the complex plane versus frequency of λ and $1/\lambda$ computed from (18). It should be noticed a monotonous phase variation in the whole frequency band. Two spirals are observed resulting in monotonous phase variations: the first one turning contra clockwise represents a positive traveling wave and the second one turning clockwise represents a negative traveling. The spirals radius of λ and $1/\lambda$ vary as:

$e^{+(L_2-L_1)\alpha}$ and $e^{-(L_2-L_1)\alpha}$ as predicted by Eq.11bis.

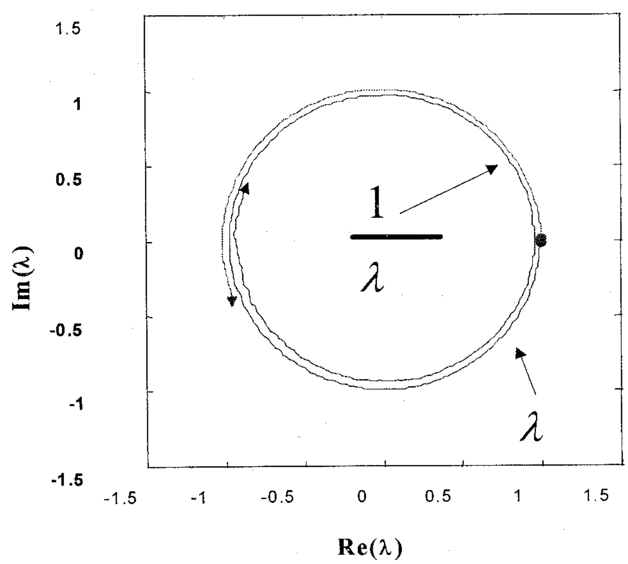

Fig. 4 Plot in the complex plane of λ and 1/λ

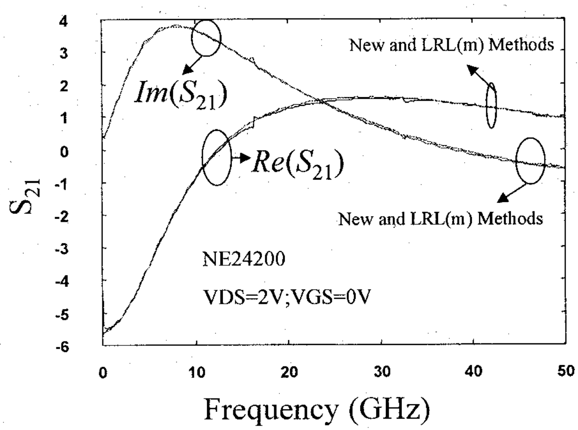

Fig. 5 Real and imaginary parts of S_{21} parameters versus frequency for the PHEMT NEC24200 measured at V_{DS}=2V

The frequency dependence of the two spiral radius indicates that the wave vanishes as frequency increases as expected in a lossy transmission line. Once λ or $1/\lambda$ is determined, S_{21} and S_{12} versus frequency is computed for each of the investigated devices.

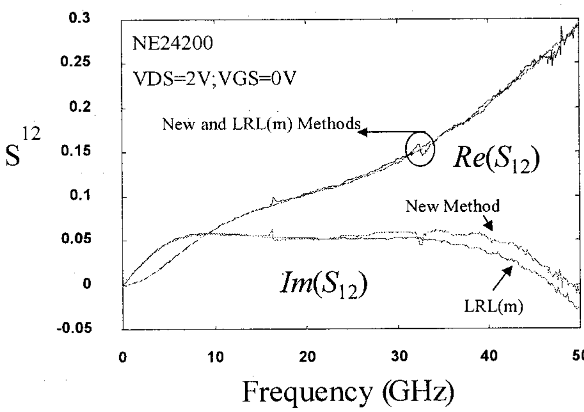

Fig. 6 Real and imaginary parts of S_{12} parameters versus frequency for the PHEMT NEC24200 measured at V_{DS}=2V and V_{GS}=0Vmeasured with *L-L* and *LRL*(m)

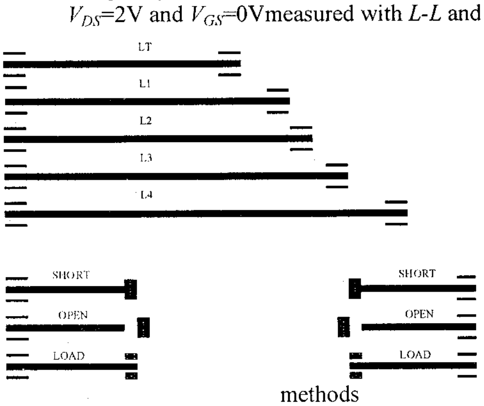

Fig. 7 Layout of the calibrations standards used for RFIC SGA-5386 and RFIC SGA-5389

Transmission scattering parameters S_{21} and S_{12} of a PHEMT (*NEC242000* biased at V_{DS} = 2 V and V_{GS} = 0 V) calculated with the *L-L* method of this work (equations (12)-(13) and (26)-(27)) and computed with the multilines (Marks R.B, 1991) *LRL* calibration technique are reported in Fig. 5. and Fig. 6. Concerning the measurement of the small signal gain of the RFIC SGA5386 and SGA5389 amplifiers, we utilize a test fixture fabricated with substrate FR4. Details of this test fixture are shown in Fig.7. Measurements of the small signal gain of these RFIC amplifiers with *L-L* and multilines *LRL* calibration techniques are reported in Fig. 8-9.

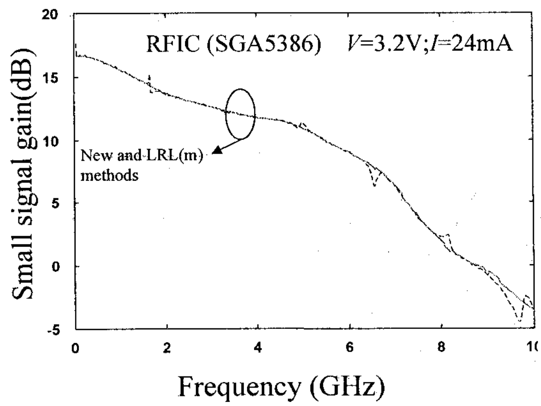

Fig. 8 Small signal gain versus frequency for the RFIC SGA-5386 measured at V=3.2V and I=24mA

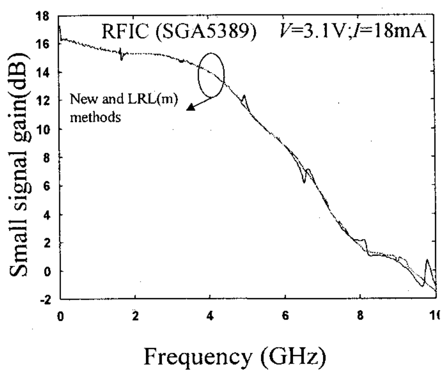

Fig. 9 Small signal gain versus frequency for the RFIC SGA-5389 measured at V=3.1V and I=18mA

It should be noticed from Fig. 5-6 and Fig. 8-9 that there are a good agreement between the S_{21} and S_{12} parameters for the PHEMT, and the small signal gain for the RFIC amplifiers, computed with L-L and with multiline methods. These results validate the accuracy of the L-L method proposed in this work.

On the other hand, plots of S_{12} and S_{21} computed using the L-M procedure (*b* and *a/c* determined with a broadband load) and *L-L* method are shown in Fig. 10-11. We observe from these plots some "spikes" in the trace of real and imaginary of S_{12} and S_{21} when they are computed with the L-L procedure. By contrast, when S_{12} and S_{21} are determined with the *L-M* procedure a free spike traces are observed. The "spikes" problem arises because the term $\left|1-\frac{b}{a/c}\right|$ is undetermined at some frequencies and this happens when the electrical length of L_2-L_1 is equal to $k\cdot180°$, $k = 0, 1, 2,..., n$. To illustrate this result in Fig. 12 we plot $\left|1-\frac{b}{a/c}\right|$ versus frequency for b and a/c determined with a 50 Ohms load and two lines.

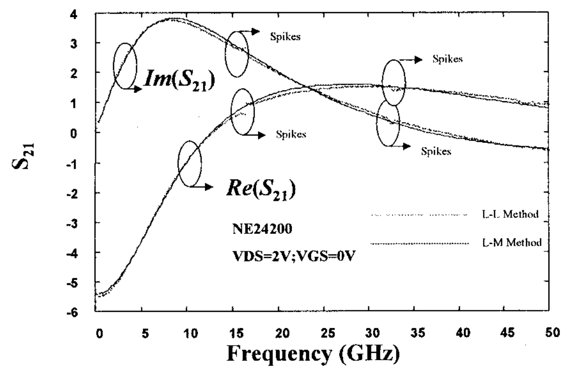

Fig. 10 Real and imaginary parts of S_{21} parameters versus frequency for the PHEMT NEC24200 measured at V_{DS}=2V and V_{GS}=0Vmeasured with *L-L* and L-M methods

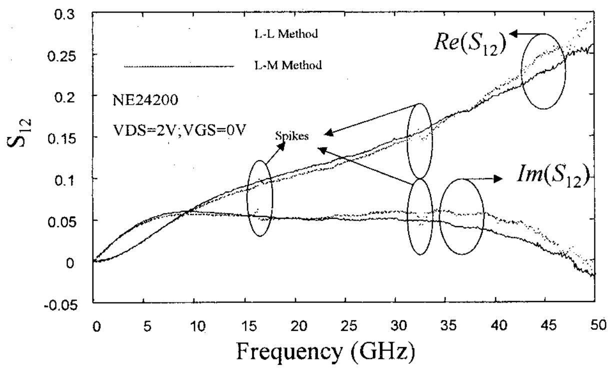

Fig. 11 Real and imaginary parts of S_{12} parameters versus frequency for the PHEMT NEC24200 measured at V_{DS}=2V and V_{GS}=0Vmeasured with *L-L* and L-M methods

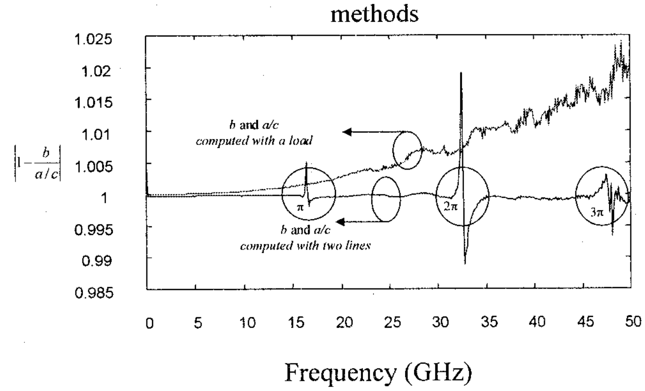

Fig. 12 Plot of $\left|1-\frac{b}{a/c}\right|$ versus frequency for b and a/c measured with *two lines* or with a match

5 Conclusions

In this paper, a new broadband de-embedding method was proposed to efficiently evaluate the S_{21} and S_{12} parameters of two-port (active or passive) using two non reflecting lines (L-L) and a line and a matched load (L-M). The main advantage of the proposed method is that nor the physical lengths nor the wave propagation constant of the lines used in the de-embedding are needed. The important variables are the b and a/c ratios and the travelling wave vector λ, which is calculated by a novel matrix approach using two non reflecting lines (L-L) or a non reflecting line and a matched load (L-M) . The λ expression in terms of b and a/c ratios allows λ, and hence S_{21} and S_{12}, to be computed in broadband. This method can be used for a fast evaluation of the transducer power gain G_T and the maximum stable gain G_{ma} of transistors and amplifiers.

Acknowledgment

The authors wish to thank José de Jesús Ibarra Villaseñor and Benjamín Ramírez Durán for device measurements. In addition, they are grateful to professor J. Graffeuil and his microwave group of LAAS du CNRS, Toulouse, France, especially J. Rayssac for transistor bonding. This work was supported by a joint funding of CICESE and CONACYT Mexico.

References

Engen G. F. and . Hoer C. A, "Thru-reflect-line: An improved technique for calibrating the dual six-port automatic network analyzer," *IEEE Trans. Microwave Theory Tech.*,vol. MTT-27, no.12, pp. 987-993, December 1979.

Eul H. J. and Schieck B., "Thru-match-reflect: One result of a rigorous theory for de-embedding and network analyzer calibration," in *Proc. 18th European* september,1988.

Marks R. B, " A Multiline method of network analyzer calibration," *IEEE Trans. Microwave Theory Tech.*,vol. MTT-39, no. 7, pp. 1205-1215, July 1991.

J. A. Reynoso-Hernández, C. F. Estrada-Maldonado, T. Parra, K. Grenier, and J. Graffeuil, "An improved method for the wave propagation constant γ estimation in broadband uniform millimeter-wave transmission line," *Microwave and Optical Technology Lett.*, vol. 22, no. 4, pp. 268-271, August 1999.

J. A. Reynoso-Hernández, C. F. Estrada-Maldonado, "Broadband determination of two-port transmission (S_{21},S_{12}) parameters of PHEMT's embedded in transmission lines," *55th Automatic RF Techniques Group Conference, pp.49-52,* Boston, Massachusetts June 15-16, 2000.

M. Q. Lee and S. Nam, "An accurate broadband measurement of substrate dielectric constant," *IEEE Microwave and Guided Wave Lett.*, vol. 6, no. 4, pp. 168-170, April 1996.

Wan Ch., Nauwelaers B, and Raedt W, "A simple correction method for two-port transmission parameter measurement," *IEEE Microwave and Guided Wave Lett.*, vol. 8, no. 2, pp. 58-59, February 1998.

J. Apolinar Reynoso-Hernández, *he received the Electronics and Telecommunications Engineering degree, M. Sc. degree in Solid State Physics and Ph. D. degree in Electronics, from ESIME-IPN, Mexico, CINVESTAV-IPN, Mexico and Université Paul Sabatier-LAAS du CNRS, Toulouse, France, in 1980, 1985 and 1989 respectively. Since 1990 he has been a researcher at the Electronics and Telecommunications Department of CICESE in Ensenada, B. C., Mexico. His research activities are concerned with physical device modeling, accurate microwave and millimeter wave measurements techniques for active device characterization and model parameter extraction. Dr. Reynoso-Hernández is member of editorial board of the IEEE Transaction on Microwave Theory and Techniques.*